Supporting Information

Tai et al. 10.1073/pnas.1411131111

SI Materials and Methods

Acute Dissociation of Cortical Neurons. Neurons from neocortex were acutely dissociated from postnatal day (P) 20–22 mice using standard procedures (1, 2). The cell suspension was placed in a 35-mm tissue-culture dish mounted on the microscope stage. After the cells were allowed to settle for 5 min, the solution was changed to an extracellular recording solution containing 20 mM NaCl, 116 mM glucose, 10 mM Hepes, 1 mM $BaCl_2$, 2 mM $MgCl_2$, 55 mM $CsCl_2$, 1 mM $CdCl_2$, 1 mM $CaCl_2$ and 20 mM tetraethylammonium chloride, adjusted to pH 7.35 with NaOH.

Patch Clamp Recordings. Whole-cell patch-clamp recordings were carried out at room temperature using an Axopatch 200B amplifier (Axon Instruments) with PCLAMP 6 software (Axon Instruments) in voltage-clamp configuration. Cell capacitance (C_m) was calculated from $C_m = Q/V$, where Q is the charge measured by integrating the capacitative current evoked by a hyperpolarizing 10-mV voltage step from a holding potential of −70 mV. Capacitative currents were minimized using the amplifier circuitry. We routinely used 70% prediction and 90% series resistance compensation. The remaining linear capacity and leakage currents were eliminated by P/4 subtraction. The intracellular solution contained 177 mM *N*-methyl-D-glucamine, 40 mM Hepes, 4 mM $MgCl_2$, 10 mM EGTA, 1 mM NaCl, 25 mM phosphocreatine-Tris, 2 mM ATP-Tris, 0.2 mM Na_2GTP, and 0.1 mM leupeptin, adjusted to pH 7.2 with H_2SO_4. Conductance–voltage (G–V) relationships (activation curves) were calculated according to $G = I_{Na}/(V - E_{Na})$, where I_{Na} is the peak Na^+ current measured at potential, V, and E_{Na} is the extrapolated equilibrium potential. Normalized activation curves were fit to Boltzmann relationships of the form $y = 1/\{1 + \exp[(V - V_{1/2})/k]\}$, where y is normalized sodium conductance, V is the membrane potential, $V_{1/2}$ is the voltage of half-maximal activation, and k is a slope factor. Analyses were carried out using Igor Pro-6.0 (Wavemetrics) and pCLAMP (Axon Instruments).

1. Yu FH, et al. (2006) Reduced sodium current in GABAergic interneurons in a mouse model of severe myoclonic epilepsy in infancy. *Nat Neurosci* 9(9):1142–1149.
2. Kalume F, Yu FH, Westenbroek RE, Scheuer T, Catterall WA (2007) Reduced sodium current in Purkinje neurons from Nav1.1 mutant mice: Implications for ataxia in severe myoclonic epilepsy in infancy. *J Neurosci* 27(41):11065–11074.

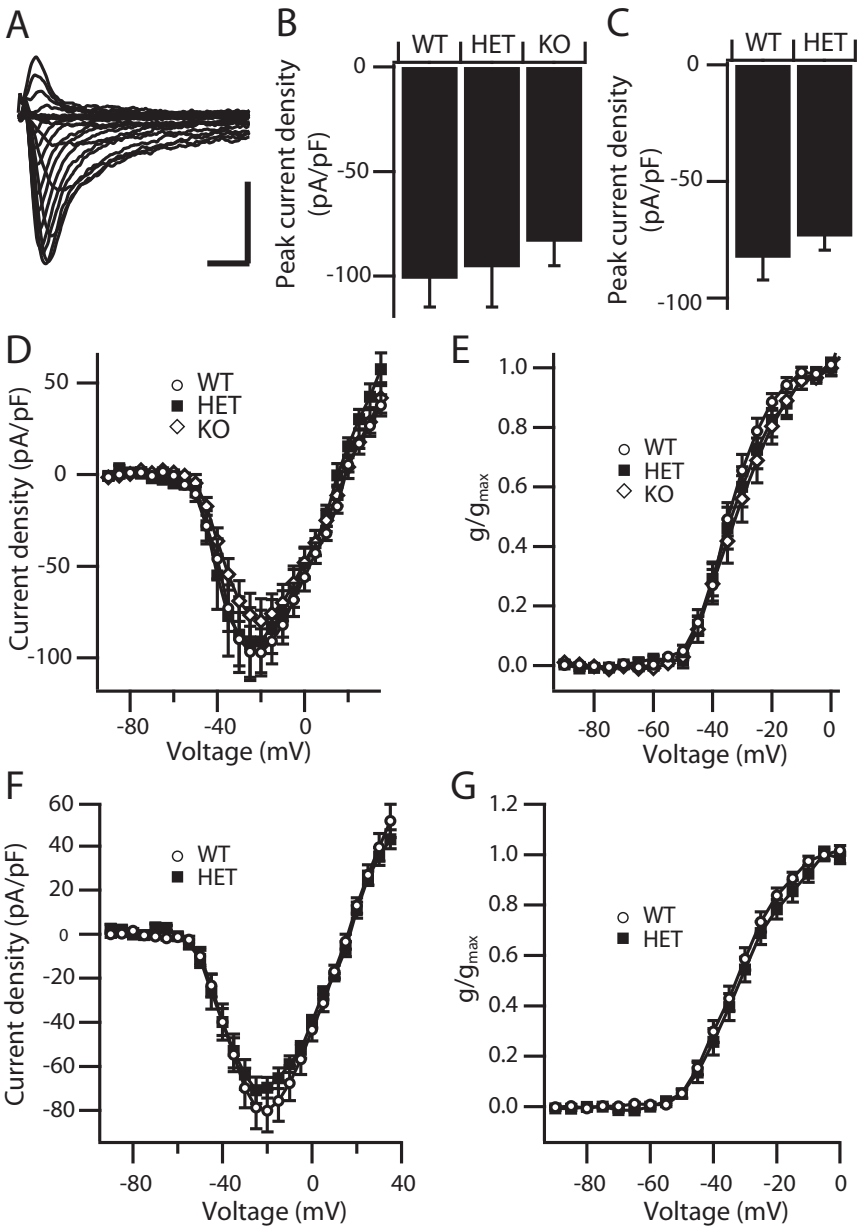

Fig. S1. Voltage-clamp recordings of sodium currents in acutely dissociated cortical interneurons from WT and $Na_V1.1$ heterozygous (HET) animals (aged P14 and P21). (*A*) Sample current traces evoked in a dissociated interneuron (P21) with a series of 20-ms depolarizations from a holding potential of −90 mV to potentials ranging from −90 to +30 mV in 5-mV increments. (Calibration: 1 ms, 1 nA.) (*B*) Mean peak current densities for dissociated interneurons (P14) of WT, HET, and KO animals (−101.17 ± 13.56 pA/pF in WT vs. −95.76 ± 19.13 pA/pF in HET, $P = 0.32$ vs. −83.53 ± 11.48 pA/pF in KO, $P = 0.17$). (*C*) Mean peak current densities for dissociated interneurons (P21) of WT and HET animals (−82.63 ± 9.55 pA/pF in WT vs. −73.53 ± 5.85 pA/pF in HET, $P = 0.57$). (*D*) Current–voltage relationships for peak sodium current of WT, HET, and KO animals (P14). (*E*) Mean conductance–voltage relationships for peak sodium current of WT, HET, and KO animals (P14). (*F*) Current–voltage relationships for peak sodium current of WT and HET animals (P21). (*G*) Mean conductance–voltage relationships for peak sodium current of WT and HET animals (P21). Values shown are expressed as mean ± SEM.

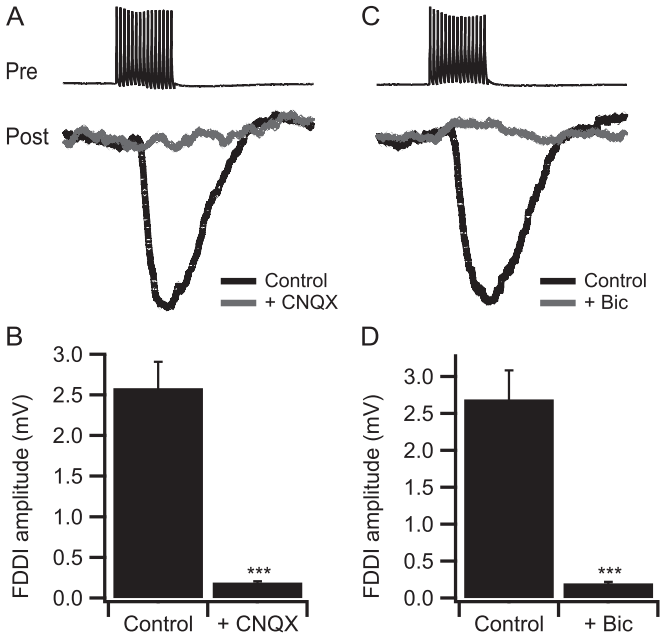

Fig. S2. Frequency-dependent disynaptic inhibition (FDDI) is blocked by both 6-cyano-7-nitroquinoxaline-2,3-dione (CNQX) and bicuculline. (*A*) Sample traces showing a train of 15 action potentials (APs) at 70 Hz in one pyramidal neuron (Pre) that triggered an FDDI signal in a neighboring pyramidal neuron (Post), which was completely blocked by CNQX (10 μM). (*B*) Amplitude of FDDI before (Control) and after application of CNQX (+ CNQX). Control: 2.69 ± 0.39 mV, + CNQX: 0.20 ± 0.02 mV; $n = 4$; ***$P < 0.001$. (*C*) Sample traces showing that a train of 15 APs at 70 Hz in one pyramidal neuron (Pre) triggered an FDDI signal in a neighboring pyramidal neuron (Post), which was completely blocked by bicuculline (+Bic; 10 μM). (*D*) Amplitude of FDDI before (Control) and after application of bicuculline (+ Bic). Control: 2.58 ± 0.32 mV, + Bic: 0.19 ± 0.02 mV; $n = 4$; ***$P < 0.001$.

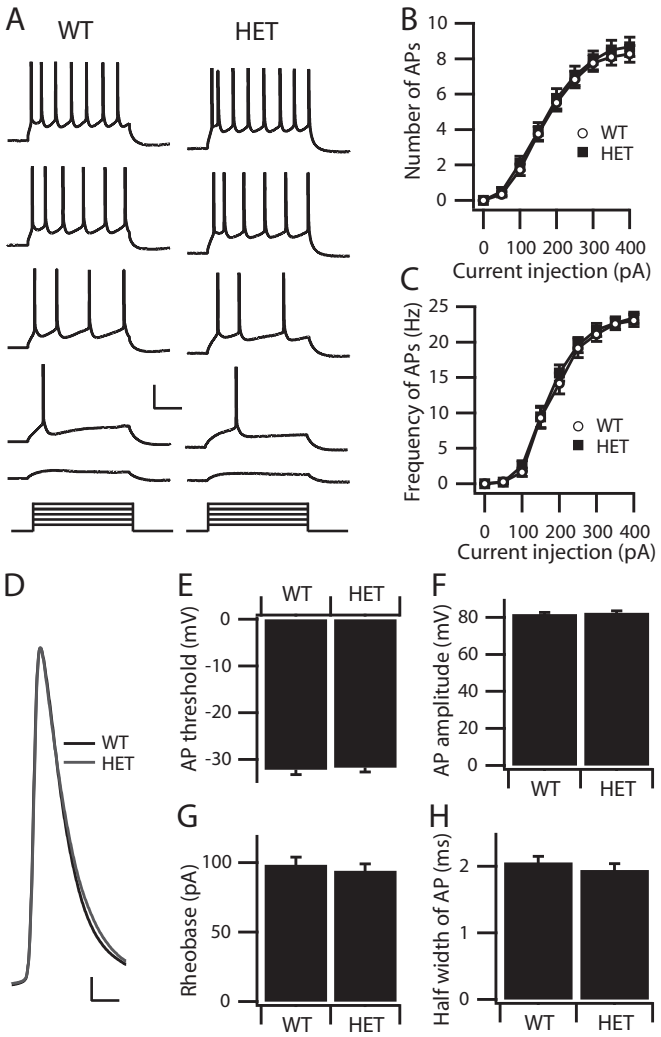

Fig. S3. Excitability of cortical layer V pyramidal neurons. (*A*) Sample traces of whole-cell current-clamp recordings in response to incremental steps of current injections (1 s, ranging from 50–450 pA), in a WT and a HET pyramidal neuron. (Calibration: 0.5 s, 50 mV.) (*B* and *C*) The number (*B*) and averaged frequencies (*C*) of APs at each step (from 0–500 pA) for WT ($n = 35$) and HET ($n = 35$) cells are plotted. (*D–H*) Properties of individual APs of WT and HET layer V pyramidal neurons. (*D*) Expanded and superimposed individual APs from recordings of the WT and HET pyramidal neurons in *A*. (Calibration: 1 ms, 10 mV.) (*E*) Mean AP threshold. WT: −32.1 ± 1.0 mV; HET: −31.7 ± 1.7 mV ($P = 0.72$). (*F*) Mean AP amplitude. WT: 81.8 ± 0.9 mV; HET: 82.6 ± 1.7 mV ($P = 0.46$). (*G*) Mean AP rheobase. WT: 98.6 ± 5.5 pA; HET: 94.3 ± 5.0 pA ($P = 0.43$). (*H*) Mean AP half width. WT: 2.05 ± 0.09 ms; HET: 1.95 ± 0.09 ms ($P = 0.29$).